

Personal Identification Based on Iris Texture Analysis using Semivariogram and Correlogram Functions

Oswaldo S. S. Junior, Zair Abdelouahab, Aristófanés CorrLa Silva

Federal University of Maranhão-UFMA, Av. dos Portugueses, SN, Campus do Bacanga
Bacanga 65085-580, São Luis, MA, Brazil

In this paper, a method for testing two geostatistics functions to extract features of the iris is proposed. The use of these kinds of functions is a good choice to discriminate information of the iris texture because they can perform analyses in any direction and at any distance. We consider the following phases: iris localization that uses three techniques: Watershed, Hough Transform and Active Contours; features extraction that use two geostatistics functions where the first is known as semivariogram and the second is known as correlogram; classification that uses the Euclidean Distance. The tests are carried out with an iris database, known as CASIA which contains 756 images. The results obtained with the localization method, as well as the results obtained by means of features classification are promising. The iris localization method has reached 90% of success. The two analyzed functions have provided above 95% of classification success. The Semivariogram function has obtained 97.35% of success while the correlogram function has obtained 97.61% of success. The preliminary results of this approach are very encouraging in characterizing iris using the two geostatistics functions.

Keywords: biometric, iris recognition, geostatistical function, semivariogram, correlogram

1. INTRODUCTION

Computational systems need to identify people to allow the use of available services within a system. For this purpose, Personal Identification Methods (PIM) were devised to guarantee that just authorized personal are able to use the services available in a system.

The PIM are usually divided into three categories: Something that you own (credit card, passport, etc), something that you know (passwords, etc) and something that you are; that is known as Biometrics [1].

The first two methods present some problems, because credit cards can be lost and passwords can be forgotten. However, in the third case where physical features are used (iris [2], fingerprint [3], face [4], etc) the above problems do not happen. The reason is that features are owned and are inherent to each person, and therefore they can not be lost nor forgotten.

Biometric systems are used in common applications. According to GAO [5] and Jain *et al* [6], application groups which use biometric systems are: commercial, governmental and judicial.

Personal identification process based on biometrics needs to extract features of a person for identification, but there are some criteria to choose such features. According to Jain *et al*. [7] these criteria are: Universality, Singularity, Permanence and Mensurability.

The iris is a physical organic device with characteristics that satisfy the four conditions mentioned above. Therefore, it is a good choice to do a personal identification process based on biometrics. A curiosity

about the iris is that it has a unique pattern in such a way that a pattern of the left eye is different from the one of the right eye within the same individual.

This paper aims to present a solution for personal identification based on iris pattern recognition that is accomplished through phases of localization, feature extraction and classification. The main contribution of this work is to apply two geostatistical functions to characterize iris texture.

In the localization phase three techniques are used, Watershed, Hough Transform and Active Contours. Each technique has an essential function for obtaining a good performance of the process. In the features extraction phase we use two geostatistical functions, the first one is known as semivariogram and the second one is known as correlogram; However, to get a better extraction, we first make an enhancement in the iris texture with the objective of compensating possible problems that can occur during iris acquisition. The classification phase uses the Euclidean Distance method.

This paper is organized as follows: Section 2 shows some related works. Section 3 presents the localization method. Section 4 describes the improvement techniques used in the iris texture, as well as the techniques used to extract their features. Section 5 presents a discussion of results. The conclusions are then described in Section 6.

2. RELATED WORKS

In the literature, there are a lot of works that implement the PIM based on iris patterns. For example, Li Ma

et al. [8], uses the Hough Transform to locate the iris. In features extraction, they use a spatial filter that captures local details of the iris. In the classification phase, the Fisher linear discriminant is first used to reduce the dimensionality of the feature vector and then the nearest center classifier is adopted for classification, thus obtaining 99.43% of success in the identification.

Another known work is the Wildes's work [9] which also uses the Hough Transform in the localization phase. In the extraction phase, he builds up a Laplacian pyramid with four different resolution levels. In the classification phase, he uses the normalized correlation in different levels of the pyramid and the Fisher linear discriminant to determine the boundary that separates an iris of a single individual from the iris different individuals.

The Daugman's work [2], one of the most recognized and practical work, uses integro-differential operators to locate the iris boundaries. In features extraction, he uses 2D Gabor wavelet and measures of dissimilarity between the iris. In the classification phase, the distance of Hamming is used to calculate the correspondence between the pair of extracted features. Using his method, he obtained 99.94% of success in the identification.

The main objective of this work is to identify an iris using texture characteristic based on two Geostatistical functions. These functions (semivariogram and correlogram) are used in other areas of knowledge (for example in, geology and ecology) but not yet explored in iris identification. Our work is the first which explores these functions in this area. The results which we have obtained are promising in comparison with the works of [8] and [2].

3. IRIS LOCALIZATION

There are a lot of methods for iris localization. One of the most used method is Hough Transform, due to the geometric characteristics presented by the iris and the pupil (approximate shape of a circle) [10, 11, 9].

The iris has two circular borders: the inner border is located between the pupil and the iris and the outer border lies between the sclera (white part of the eye) and the iris.

The iris localization method is divided into three phases: edge detection, circular borders localization and eyelids extraction, (see Figure 1).

3.1. Edge Detection

This phase aims at creating the edge map which can be a difficult task since many existing objects in the image (eyelashes, eyelids, skin and the own iris texture) may generate undesirable edges, resulting in an edge map with a lot of noise.

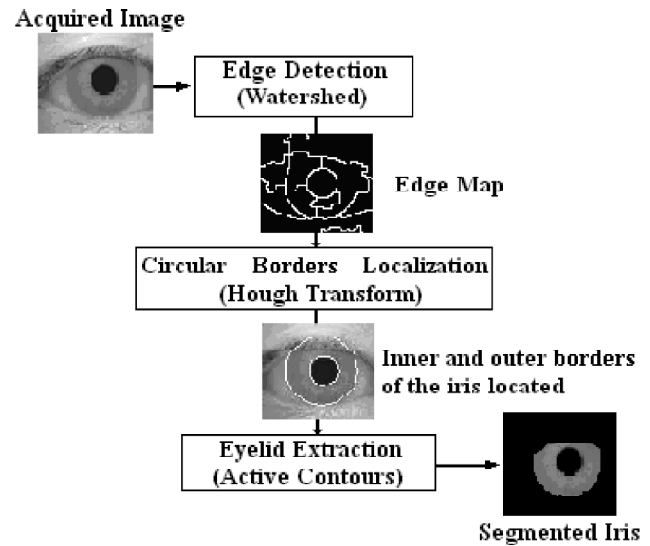


Figure 1: Scheme for iris localization

The Watershed technique [12] is used with some adaptations to create an edge map of the images. The adaptations are needed to reduce the processing time, the image overfilling in many portions and thus making its use impossible.

To avoid overfilling, it is not allowed to generate hydrographic basins in function of the number of minimum locals of the image. Instead, the candidates of minimum locals are filtered with a preprocessing algorithm so that only candidates that obey certain minimum size criteria are accepted.

The candidate filtering is initiated with the search of lower intensity points. For each one of them, a region growing algorithm is executed to measure the associated basin area size. If the area is larger than a threshold, then a Watershed seed is created.

This is necessary because iris images have, in general, a very complex texture, abundant in tone changes caused by irregularities in several image features such as in eyelashes, eyelids and the own iris.

To improve the processing time, the Watershed technique is not applied directly on original images, Figure 2a, but into reduced images with lateral dimensions equal to 25% of the original image, Figure 2b. With such miniaturization, the scale factor is chosen to ensure that in spite of possible loss of information the most important aspect (iris border) still remain characterized. This reduces the technique processing time in about 95% and generates the edge map that is used in the next phase. Figure 2c shows an edge map generated by this method.

3.2. Circular Borders Localization

To detect the iris inner and outer borders, the Hough Transform technique (HT) [13] is used. The HT uses the

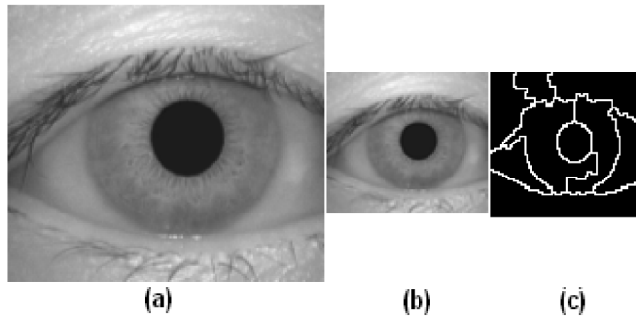


Figure 2: (a) Original image; (b) Reduced image; (c) Edge map

edge map generated in the previous phase. A good result of this phase depends on a reasonable percentage of the border that represents the circle of the iris and the pupil to be defined. This is because the HT is capable to reconstitute the borders.

To detect the iris inner border, we have used radius values¹ from 8 up to 17 pixels to fill the accumulation vector, and select the center coordinate. This process can be made due to the great contribution of the inner border in the images.

To locate the iris outer border, we have used radius values from 19 up to 35 pixels to fill the accumulation vector, but differently of the inner border case, we do not use the center that has more votes in the accumulation vector. Instead, we use a procedure described in three stages.

In the first stage, it is selected the most voted 80 center coordinates². Then in the second stage, we verify which coordinates are inside an imaginary circle centered in the pupil center, and which have a radius value 50% of pupil radius. The third stage selects the center coordinate that is closer to the pupil center. This procedure increases the number of iris found.

With the accomplishment of this procedure, the outer border localization of the iris with less borders definition is more efficient, because the iris with such characteristic usually does not get the necessary number of votes to be considered a circle found, but they are among the most voted. A fact that helps in this process is that the centers of the inner and outer borders are very close to each other.

After detecting the centers and radius, it is necessary a scale transformation to find the corresponding values in the original image, because the edge map where the HT is applied is in a different scale, as it can be seen in the Figure 2c. To find the centers of the inner and outer borders in the original scale we use the equation:

$$c_o = 4c_r + 2 \quad (1)$$

where c_o represents the center in the original scale and c_r represents the center detected with HT. A constant 2 is introduced in the Equation 1 to make the adjustment in

the transformation scale of the reduced image to find the value of the center and ray of the original image.

To find the radius in the original scale, we use:

$$r_o = 4r_r \quad (2)$$

where r_o represents the radius in the original scale and r_r represents the radius detected with the HT.

Figure 3a shows the circles of the inner and outer borders found in the reduced image and Figure 3b shows the circles after a scale transformation in the original image.

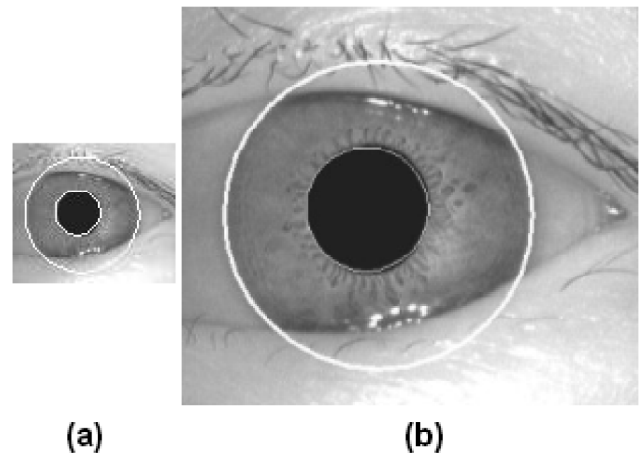


Figure 3: (a) Circles found using the HT in the edge map; (b) Circles after scale transformation

3.3. Eyelid Extraction

In this phase, the Active Contours technique [14] is used to extract the inferior and superior eyelids that cover the iris, considering that the circles of the inner and outer borders of the iris were found in the previous phase.

Initially, to exclude the eyelids, we set the snaxels (active contour points) located at a circle with the same center of the inner border of the iris and with a radius 18 pixels larger than its outer border. This procedure is necessary, because if the snaxels are on top of the inner border of the iris, the contour may have the tendency to adapt itself to the latter and not to the outer border shape of the iris.

Thus we set an outer limitation circle avoiding the active contour to cross the desired area, in cases where we have less border definition or even when we have no border. The circle that delimits the snaxels can be seen in Figure 4a and the final result of the iris localization method, in another words, the iris image without the eyelids can be seen in Figure 4b.

4. IRIS FEATURES EXTRACTION

Some factors can interfere in the iris recognition process such as parts of the human eye that are not interesting to

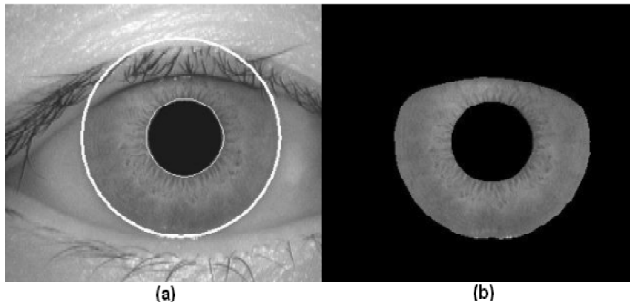


Figure 4: (a) Snaxels delimitation in circle; (b) Iris without eyelids

the process, inconsistency of dimensions due to pupil dilatation or variation of the camera distance and a non-uniform brightness caused by the light source position.

Thus, before starting the feature extraction process some procedures must be done trying to minimize these problems such as normalizing the image and improving the illumination in order that the extracted features may identify a unique person. In the next section, the accomplished improvements as well as the feature extraction technique are presented.

4.1. Iris Normalization

Two iris images, obtained in different intervals of time, hardly present the same dimensions, even if they belong to the same person. This happens due to the adverse conditions that appear in the environment where the image is captured. As an example, the illumination variation can be mentioned. It causes the pupil's size to change, resulting in the iris texture deformation. Accordingly to Li Ma *et al.* [8] elastic deformation in the iris texture may affect the results of the iris matching.

To obtain a better accuracy in the iris texture analysis, it is necessary to compensate this deformation. In general, the iris circle is mapped to a rectangular block of fixed size [2, 8]. This transformation may usually cause loss of information.

In our work, all iris images are normalized to a circular sector, to avoid the loss of information, with the same center of the inner border of the iris and with a thickness of 30 pixels. This number was determined after empirical tests with the objective to preserve the area of the Iris with excellent information. Moreover, in some cases we prevent to get undesirable information such as information of the eyelid and eyelashes.

Figure 5 indicates the iris area that we use in the analysis.

4.2. Image Enhancement

The iris image, generally, has a low contrast and may have non-uniform brightness, which is usually caused by the position of the light source in the environment where

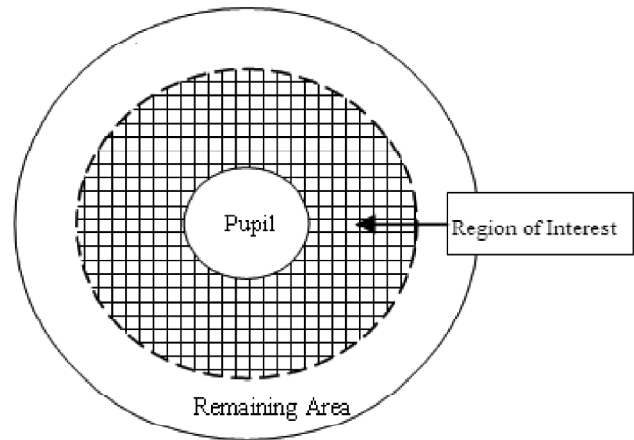


Figure 5: Region of interest the Iris

the image is captured. These factors can contribute negatively in the following stages of the process (feature extraction and iris matching).

To get a better iris texture, first the Gaussian 2D filter [15], with a mask of 3×3 is used to reduce the noise in the image. Thereafter, it is computed the complement of the filtered image. Then, the normalized image is subtracted from the complement to reduce the brightness of the image giving a stronger contrast that still is not an ideal one.

To compensate the non-uniform brightness, as well as to obtain an appropriate contrast the histogram equalization [15] is used in blocks of 15×15 , what enhances local details of the iris texture.

Figure 6 presents the normalized image and the improvement result, where it can be clearly observed that the characteristics of the iris are better depicted than in the original image.

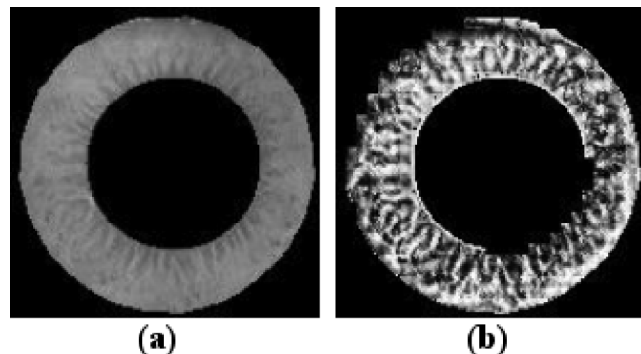


Figure 6: (a) Normalized image before improvement; (b) Normalized image after improvement

4.3. Iris Texture

Personal identification based on iris is made through analysis of its texture; therefore, it is interesting to investigate representation methods (or functions) that can analyze and extract information.

According to [16] the first and more important task in the texture analysis is to extract texture features which most completely embody information about the spatial distribution of intensity variations in an image. Thus, the application of these functions in iris recognition is an alternative, because an iris possesses an interesting structure and it provides a rich texture in information that these functions can capture. In [17] the author shows that semivariogram, one of the geostatistical functions used in this work, can be used to characterize patterns of units of texture.

Another advantage of using such functions to discriminate information on iris texture is that they can make analyses in any direction and at any distance, which is interesting in case the iris presents a very complex texture.

In practice, some of the most usual terms used by interpreters to describe textures, such as smoothness or coarseness, bear a strong degree of subjectivity and do not always have a precise physical meaning. Analysts are capable of visually extracting textural information from images, but it is not easy for them to establish an objective model to describe this intuitive concept. For this reason, it has been necessary to develop quantitative approaches to obtain texture descriptors. Thus, in a statistical context, textures can be described in terms of two main conceptual components associated to pixels (or other units): variability and spatial correlation [18]. The first component is frequently analyzed at the local level by calculating the variance, which is a statistical measure of pixel dispersion in relation to the mean value. The second characteristic, spatial correlation, assumes that pixels are not completely distributed in a random way within an image and, consequently, there exists a spatial variability (or dependence) structure associated with them. The advantage of the geostatistical approach is that both aspects can be jointly modeled, as will be discussed below.

Geostatistics [19, 20] is the analysis of spatially continuous data. It treats geographic attributes as random variables whose depend joint distributions on their locations.

The degree of similar properties shared by close neighbors over a surface is characterized by spatial autocorrelation [21]. This notion has usual applications in geostatistics and image processing.

There are some formal statistics which attempt to measure spatial autocorrelation. This includes indices, such as Semivariogram and Correlogram, which attempt to identify whether spatial autocorrelation exists between samples [22].

4.3.1. Semivariogram Function

The semivariogram function is used with success for feature extraction in several applications of different study

areas. For example, in agriculture it is used to study the soil properties [23] and in medicine it is used for medical diagnostic [24]. In this work, we intend to use it in biometrics to extract discriminating features from the iris texture.

Semivariance is a measure of the degree of spatial dependence between samples. The magnitude of the semivariance between points depends on the distance between the points. A smaller distance yields a smaller semivariance and a larger distance results in alarger semivariance. The plot of semivariances as a function of distance from a point is referred to as a semivariogram. The semivariogram function summarizes the strength of associations between responses as a function of distance, and possible direction [20]. We typically assume that spatial autocorrelation does not depend on where a pair of observations (in our case, pixel) is located, but only on the distance between the two observations, and possibly in the direction of their relative displacement.

A semivariogram function has three main features: sill, range, and nugget (Figure 7). A sill is the ordinate value at which the semivariogram level is off, that is, its an asymptotic value; the range is the distance at which this leveling off occurs, that is, the spatial extent of the structure in the data; and the nugget is the semivariance at a distance 0.0, that is, the interception with the Y axis. A nonzero nugget can imply either intrinsic variability in the data (the component typically described as “sampling error”), or it might indicate that the sampling is conducted at an inappropriate spatial scale, that is, there is considerable variability of scales smaller than the smallest between distance-points.

The semivariogram function is defined by

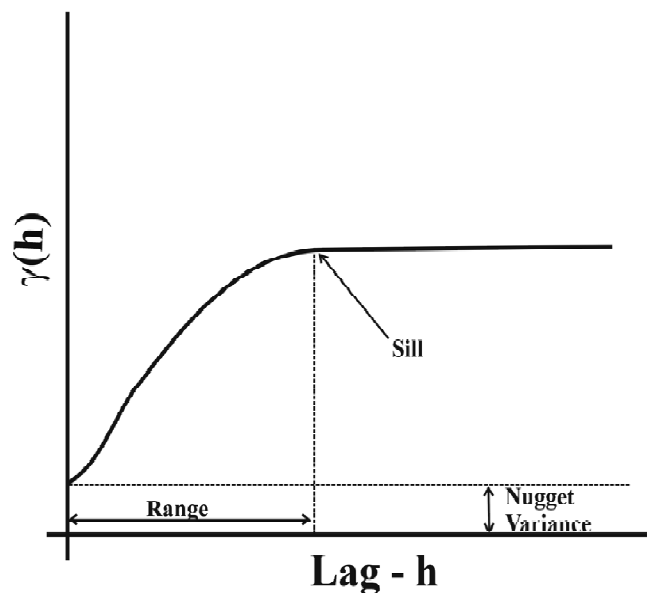


Figure 7: Semivariogram and its main features: range, sill, and nugget

$$\gamma(h) = \frac{1}{2N(h)} \sum_{i=1}^{N(h)} (x_i - y_i)^2 \quad (3)$$

where h is the lag (vector) distance between the head value (target pixel), y_i , and the tail value (source pixel), x_i , and $N(h)$ is the number of pairs at lag h .

When computing directional experimental semivariograms in 2D, azimuth angle is used to define the direction vector. To define the rotation of a vector, we assume that the unrotated vector starts in the $+y$ direction. The azimuth angle is the first angle of rotation and it represents a clockwise rotation in the horizontal plane starting from the $+y$ axis. Other parameters used for semivariogram calculations such as lag space, lag tolerance, direction, angular tolerance, maximum bandwidth are exemplified in Figure 8.

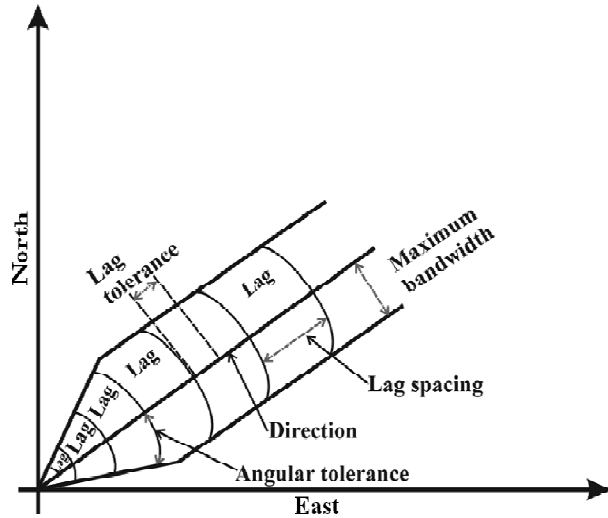


Figure 8: Parameters used for semivariogram calculations

4.3.2. Correlogram Function

A correlogram function or correlation function is the relationship between the correlation coefficient of a scatterplot and a distance h . This function can be summarized as the normalized version of the covariogram function [25] and the correlation coefficients are in the strips from -1 to 1.

A correlogram presents high results for small distances and tends to present low results when the distance increases, in other words, the correlation is high for units close to each other and tends to zero when the distance between them increases.

A correlogram function is defined by

$$\rho(h) = \frac{C(h)}{\sigma_{-h}\sigma_{+h}} \quad (4)$$

where σ_{-h} is the standard deviation of the vectors' origin values,

$$\sigma_{-h} = \left[\frac{1}{N(h)} \sum_{i=1}^{N(h)} x_i^2 - m_{-h}^2 \right]^{\frac{1}{2}} \quad (5)$$

and σ_{+h} is the standard deviation of the vectors' extremities values,

$$\sigma_{+h} = \left[\frac{1}{N(h)} \sum_{i=1}^{N(h)} y_i^2 - m_{+h}^2 \right]^{\frac{1}{2}} \quad (6)$$

$N(h)$ is the number of pairs at lag h , x_i is source pixel, y_i is target pixel, m_{-h}^2 is average of x_i and m_{+h}^2 is average of y_i .

5. EXPERIMENTAL RESULTS

The iris database used in this work is known as CASIA [26]. It has approximately 756 images divided in 108 classes, where each class has 7 iris samples with 320×280 pixels in gray level. The radius of the iris from database vary between 87 and 113 pixels which, according to Daugman [2], is a good number because he states that a device should supply at least 70 pixels in the radius of the iris to capture the details.

All tests are carried out with all database images. The whole process is implemented using the programming language known as Java and tested on a computer Pentium IV with 3.0 GHz and 512 MB RAM memory.

The results are presented in two sections: the first presents the iris localization results and the second shows the matching results.

5.1. Iris Localization Results

The iris localization is done in three phases as described in Section 3. The results of each phase are discussed below.

The first phase aims at generating the edge map using the Watershed technique. The results are good for this application because the edge map do not present noise excess caused by undesirable objects found in the majority of tested images. The adaptations done in the technique reduced the processing time, but it still continues high, on average 2 seconds.

The second phase detects the circles of the inner and outer iris border. The use of the HT technique leads to promising results. This is because edge maps that are used in the process usually have presented a low incidence of noise which contributes to a better performance of this phase. The average time to locate the circles is about 0.5 seconds and the rates of the success to find the inner and outer borders of the iris are respectively, 98% and 90%. The cases where the inner and outer borders are not found are due to little contribution of the circle borders. An example can be seen in the Figure 9a.

The last phase aims at extracting the eyelids that possibly come together with the iris. The results using the Active Contours technique are promising reaching 90% of success in a medium time of 0.3 seconds. The extraction has not been successful when the eyelids are covered or when they are much close to the inner border of the iris and when the eyelids borders are not well defined. A case where the eyelids extraction has not been successful, because it is very close to the inner border is presented in Figure 9b.

The proposed iris localization method has reached a good precision getting 90% of success with a total processing time that varies between 2 and 3 seconds.

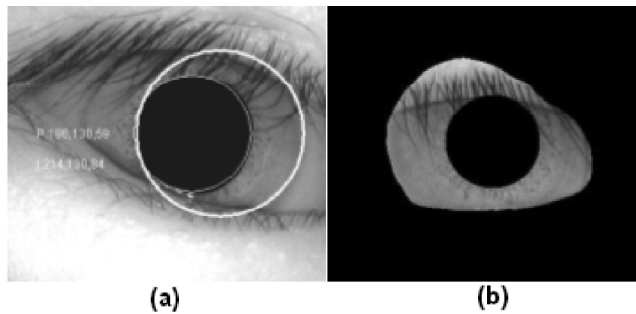


Figure 9: (a) Wrong iris localization; (b) Wrong eyelids extraction

5.2. Matching Results

To obtain a better precision in the process of features extraction, the image presented in Figure 6b is divided in 120 circular sectors, where in each one the semivariogram and correlogram functions are calculated. This number of sectors was defined to capture the local details of the iris texture.

The parameters used by the semivariogram and correlogram functions for features extraction in each sector are the directions 0° , 45° , 90° and 135° with angular tolerance of 22.5° and only 2 lags with lag spacing equal to 1 and lag tolerance equal to 0.5.

To create the Features Vector (FV), we have extracted 8 features for each circular sector, two in each direction, generating a total of 960 features.

In the classification, the Euclidean Distance (ED) is used due to the nature of the extracted features and is computed by:

$$ED(A, B) = \sqrt{\sum_{f=1}^k (N(A_f) - N(B_f))^2} \quad (7)$$

where $N(A_f)$ and $N(B_f)$ are, respectively, the normalized features of a known iris and of an unknown iris, k represents the number of features. The normalization is defined by

$$N(X) = \frac{X - \bar{X}}{\sigma} \quad (8)$$

where X , \bar{X} and σ are respectively the original feature, mean and standard deviation of FV.

The objective is to compare the degree of similarity between the iris represented by A and B. The similarity between iris depends on the distance between them. A smaller distance yields a larger similarity and a larger distance results in a smaller similarity.

A biometric recognition system can be classified into two different modes: identification and verification. The identification is the process where an individual FV is compared with n other FVs stored in a database. The verification or authentication is the process where an individual FV is only compared with its own FV registered previously in the database. The enrollment (FV) is recovered through a user name.

To accomplish the tests, with the mode of identification and verification, all images of the database are considered, including the images with a wrong segmentation. This is possible because most of segmentation errors result from wrong eyelids exclusions. The errors are compensated in the normalization phase where the area of interest of the iris is obtained. It is also considered the Mean Features Vector (MFV) for each one of the 108 iris classes of the database. The MFV is obtained by calculating the means among the FV from each iris belonging to the same class.

In the verification mode, the tests are made through authentication simulations, where a threshold (t) is used to indicate the similarity degree. A total of 81,648 simulations are carried out for each value of t in an interval varying from 0 to 1 with an increment of 0.04. This means that for each value of t all 756 FV of the database are compared with all of the 108 MFV. From these simulations, it is possible to generate a system error rates that measures their precision: FAR (False Acceptance Rate) and FRR (False Rejection Rate) [27, 11].

Figure 10 represents the analysis of two error rates (FAR and FRR) for each value of t using the semivariogram function. This analysis is called threshold analysis and it is useful to check the EER (Equal Error Rate) which represents the intersection point of the two curves. The EER is used to compare biometric systems where smaller values indicate that the system is better than with larger values. The EER values calculated in this work are 0.0278 or 2.78% using the semivariogram function and 0.03 or 3% using the correlogram function.

The curve ROC (Receiver Operating Characteristic) is built with the FAR and FRR values. This curve is useful

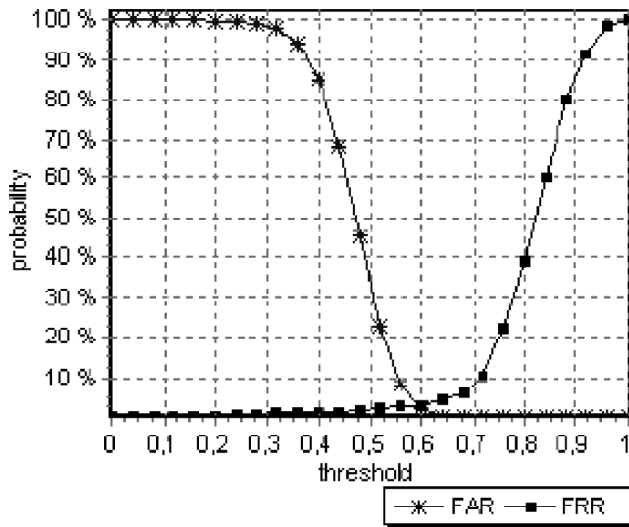


Figure 10: Error rates (FAR x FRR) using semivariogram function

to represent systems accuracy where a system that has a curve nearer to the origin is better. Figure 11 shows the ROC curves for each one of the geostatistical functions used in this work, where in the same figure we can see in detail that the semivariogram function has obtained a better result than the correlogram function; however both of them have reached a good result.

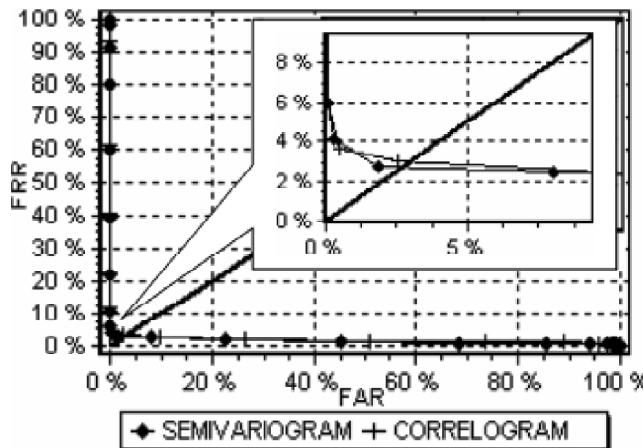


Figure 11: ROC curve of the correlogram and semivariogram functions

In the identification mode, the FV of an iris is compared, using Equation 7, with all the other 108 MFV, resulting in a distance for each comparison. The objective of this test is to prove that the comparison between FV of an iris and MFV of the group to which it belongs is smaller than any other comparison between itself and the other 107 MFV. This test is carried out for all irises of the database resulting in a success of 97.35% using the semivariogram and 97.61% using the correlogram. The tests where the iris are not identified correctly occur due to problems mentioned in the section 5.1. Figure 12 shows

the comparison of FV of the identified iris for 051_2_4, in the iris database (CASIA), with all other 108 MFV using the correlogram function, where the smallest value which is found belongs to the group 051.

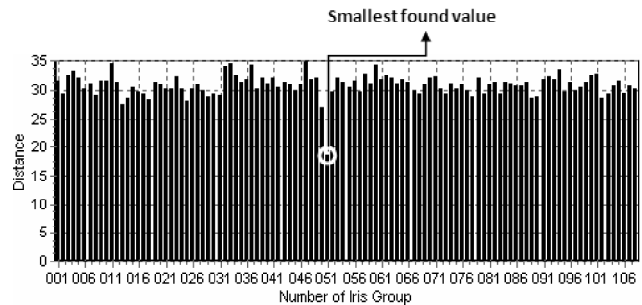


Figure 12: Comparison of FV of the iris (051_2_4) with all other 108 MFV using correlogram function

6. CONCLUSION

A biometric identification technique based on pattern of human iris has been reported. This technique is well suited to any access control system which requires high level security. The processing algorithms as well as the feature extraction block and the verification system have been described.

The iris localization uses Watershed algorithm, Hough Transform and Active Contours as pre-processing phases followed by phases of feature extraction block and system verification. The localization phase has obtained about 90% of success rate.

A major approach for iris recognition today is to generate feature vectors corresponding to individual iris images and to perform iris matching based on some distance metrics. One of the problems in feature-based iris recognition is that matching performance is significantly influenced by many parameters in feature extraction process, which may vary depending on environmental factors of image acquisition. We present a scheme of feature extraction based on two geostatistical function: semivariogram and correlogram. The semivariogram function has obtained 97.35% of success rate, and correlogram function has obtained 97.61% of success rate. The applications these two functions are our main contribution.

In future, we intend to test the proposed method with other databases with larger number of iris samples that can present more complex cases. Another work planned is to study how to improve the performance of iris localization.

NOTES

1. The radius values used to fill the accumulation vector are determined through a study done with the database.
2. Some tests were made to choose this number.

REFERENCES

- [1] O. S. S. Junior, Método de reconhecimento pessoal através da íris usando funções geoestatísticas, Master's thesis, Universidade Federal do Maranhão, São Luís (04/12/2006 2006).
- [2] J. Daugman, How iris recognition works., *IEEE Transactions on Circuits and Systems for Video Technology*, **14** (1), (2004), 21–30.
- [3] J. Li, W. Y. Yau, H. Wang, Combining singular points and orientation image information for fingerprint classification, *Pattern Recogn.* **41** (1), (2008), 353–366.
- [4] J. M. R. T. Fernando J. S. Carvalho, Detecção de faces em imagens baseadas na identificação da pele e dos olhos, T´ekhne - Revista de Estudos, *Politécnicos*, **6** (9), (2008), 245–266.
- [5] GAO, Information security: Challenges in using biometrics., The Century Foundation, [Online]. Available: <http://www.tcf.org/list.asp?type=RR&pubid=462>, 21–10–2008.
- [6] A. K. Jain, A. Ross, S. Prabhakar, An introduction to biometric recognition., *IEEE Transactions on Circuits and Systems for Video Technology*, **14** (1), (2004), 4–20.
- [7] A. K. Jain, S. Pankanti, S. Prabhakar, Biometric Recognition: security and privacy concerns, *IEEE Security & Privacy*, **1** (1), (2003), 33–42.
- [8] L. Ma, T. Tan, Y. Wang, D. Zhang, Personal identification based on iris texture analysis, *IEEE Trans. Pattern Anal. Mach. Intell.*, **25** (12), (2003), 1519–1533.
- [9] R. Wildes, Iris recognition: An emerging biometric technology., *Proceedings of the IEEE*, **85** (9), (1997), 1348–1363.
- [10] W. Kong, D. Zhang, Accurate iris segmentation based on novel reflection and eyelash detection model, Intelligent Multimedia, Video and Speech Processing, 2001. Proceedings of 2001 International Symposium on (2001), 263–266.
- [11] L. Masek, Recognition of human iris patterns for biometric identification, Tech. rep., School of Computer Science and Software Engineering, The University of Western, Australia (2003).
- [12] J. B. T. M. Roerdink, A. Meijster, The watershed transform: Definitions, algorithms and parallelization strategies, *Fundamenta Informaticae*, **41** (1-2), (2000), 187–228.
- [13] R. M. Hadad, J. Paulo P. Martins, A. de Albuquerque Araújo, Using the hough transform to detect circular forms in satellite imagery, in: SIBGRAPI '01: Proceedings of the 14th Brazilian Symposium on Computer Graphics and Image Processing, IEEE Computer Society, Washington, DC, USA, 2001, 406.
- [14] F. Leymarie, M. D. Levine, Tracking deformable objects in the plane using an active contour model, *IEEE Transactions on Pattern Analysis and Machine Intelligence*, **15**(6), (1993), 617–634.
- [15] M. Šonka, V. Hlaváč, R. D. Boyle, Image Processing, Analysis and Machine Vision, 1st Edition, Chapman and Hall, London, UK, 1993.
- [16] A. Kourgli, A. Belhadj-aissa, Texture primitives description and segmentation using variography and mathematical morphology., in: SMC (7), *IEEE*, 2004, 6360–6365.
- [17] A. Kourgli, A. Belhadj-aissa, Characterising textural primitives using variography, Proc. IMVIP 2000, Belfast, Ireland, (2000) 165–175.
- [18] R. Gonzalez, R. Woods, Digital Image Processing, Second Edition, Prentice Hall, 2002.
- [19] A. G. Journel, C. J. Huijbregts, Mining Geostatistics, Academic Press, London, 1978.
- [20] I. Clark, Practical Geostatistics, Applied Science Publishers, London, 1979.
- [21] D. A. Griffith, Distributional properties of georeferenced random variables based on the eigenfunction spatial filter, *Journal of Geographical Systems*, **6** (2004), 263–288(26).
- [22] F. M.-J. L. P. M. D. R. M. Mark RT, Dixon DP, Conceptual and mathematical relationships among methods for spatial analysis, *Ecography*, **25**, (2002), 558–577.
- [23] R. Ferreyra, H. Apezteguia, R. Sereno, J. Jones, Reduction of soil water spatial sampling density using scaled semivariograms and simulated annealing, *Geoderma*, **110**, (2002), 265–289.
- [24] A. C. Silva, P. E. F. Jr., P. C. P. Carvalho, M. Gattass, Diagnosis of lung nodule using the semivariogram function., in: SSPR/SPR, 2004, pp. 242–250.
- [25] E. H. Isaaks, R. M. Srivastava, An Introduction to Applied Geostatistics, Oxford University Press, Inc, 1989.
- [26] CASIA, iris image data base., Institute of Automation, Chinese Academy of Sciences, [Online]. Available: <http://www.sinobiometrics.com>, 15–07–2007 .
- [27] R. Ives, A. Guidry, D. Etter, Iris recognition using histogram analysis, Signals, Systems and Computers, 2004. Conference Record of the Thirty-Eighth Asilomar Conference on **1**, (2004), 562–566.